

## Identification of Amino Acids at Two Dimer Interface Regions of the $\alpha$ -Factor Receptor (Ste2)<sup>†</sup>

Hong X. Wang and James B. Konopka\*

*Department of Molecular Genetics and Microbiology, Stony Brook University, Stony Brook, New York 11794-5222*

*Received March 11, 2009; Revised Manuscript Received June 2, 2009*

**ABSTRACT:** The yeast  $\alpha$ -factor pheromone receptor (Ste2) belongs to the large superfamily of G protein-coupled receptors (GPCRs) that characteristically contain seven transmembrane domains (TMs). A wide range of GPCRs are thought to exist as dimers or oligomers. To identify the interface regions that mediate oligomerization of Ste2, a set of 73 different mutants with Cys residues substituted near the extracellular ends of the transmembrane domains were screened for the ability to form intermolecular disulfide bonds. Disulfide bonds formed between Cys residues at six positions in Ste2. Cys substituted for Val-45 formed disulfide bonds, indicating contact between residues at the extracellular end of TM1. Disulfide bonds also formed with Cys residues substituted for five different residues clustered near the extracellular end of TM4 (Val-183, Val-186, Lys-187, Met-189, and Ile-190). Binding of the  $\alpha$ -factor ligand to Ste2 did not change the sites at which cross-linking occurred in these TMs, but it did increase the efficiency of dimer formation for the Ste2-V183C mutant. Interestingly, oligomers of the class A family of vertebrate GPCRs are also thought to form homomeric contacts at TM1 and TM4. These results support the conclusion that GPCRs form oligomers and not just dimers, since TM1 and TM4 are too far apart in the class A GPCRs to form contacts in the same dimer moiety. Similar dimer interface sites in Ste2 and class A receptors provide further evidence that many aspects of structure and function are highly conserved across the divergent GPCR superfamily.

G protein-coupled receptors (GPCRs)<sup>1</sup> transduce the signals for a wide range of stimuli, including light, taste, olfaction, and many biomedically important hormones. GPCRs function by activating the  $\alpha$ -subunit of heterotrimeric G proteins to bind GTP and induce cellular signaling pathways. GPCRs also share a similar structural organization in that they are composed of a bundle of seven transmembrane domains (TMs) connected by extracellular and intracellular loops (1, 2). Interestingly, in spite of these similarities, GPCRs have divergent sequences and have been grouped into at least five distinct classes with no obvious sequence similarity between the receptors in the various classes (3, 4). However, it is thought that there are underlying similarities in the mechanisms of signal transduction by members of the diverse GPCR family (5).

Another common feature of GPCRs is the ability to form dimers and in some cases higher-order oligomers (6). The ability to form homodimers or heterodimers between two different GPCRs has been implicated in diverse receptor functions, including biogenesis, plasma membrane targeting, and signaling (6–9). Some GPCRs are also thought to form higher-order oligomers. For example, oligomer formation of rhodopsin, a prototypical class A GPCR, was proposed on the basis of a membrane packing arrangement observed using atomic force

microscopy (10, 11) and electron cryomicroscopy (12). Cross-linking studies also indicate that rhodopsin and other class A GPCRs form oligomers (13–16). In spite of the widespread evidence of GPCR oligomerization, the function of this type of intermolecular interaction is not consistently defined across the GPCR superfamily. Members of the class C family of GPCRs are thought to form homo- or heterodimers, but not higher-order oligomers (17). There is also evidence that monomers of rhodopsin (18) and the  $\beta$ -adrenergic receptor (19) can signal efficiently.

Sites of interaction between GPCR monomers are being defined to improve our understanding of the structural arrangement of oligomers. One approach that has been successful for identifying the dimer interface regions is to determine if Cys residues substituted into different regions of GPCR monomers are sufficiently close in space to form a disulfide-bonded dimer. These studies are based on Cys cross-linking approaches that have been very successful for mapping the TM orientations of other membrane proteins, including bacterial chemotaxis receptors and the lacY lactose permease (20–22). Application of these approaches to class A GPCRs has implicated residues in TM1, TM4, and TM5 as contact regions in oligomers (13–15). To test whether the oligomer interface regions were conserved in a more divergent GPCR, we examined the *Saccharomyces cerevisiae*  $\alpha$ -factor pheromone receptor (Ste2), which was previously implicated in the formation of dimers or oligomers by FRET and BRET studies (9, 23–25). Ste2 is well-suited for this type of cross-linking analysis because it lacks essential Cys residues and does not form an intramolecular disulfide bond between the second extracellular loop and TM3 that is present in many other GPCRs. Contact sites at the oligomer interface of Ste2 were identified by

<sup>†</sup>This work was supported by a grant from the American Heart Association awarded to J.B.K.

\*To whom correspondence should be addressed. E-mail: james.konopka@sunysb.edu. Phone: (631) 632-8715. Fax: (631) 632-9797.

Abbreviations: TM, transmembrane domain; GPCR, G protein-coupled receptor; PBS, phosphate-buffered saline; CuP, Cu(II) (1,10-phenanthroline)<sub>3</sub>; FRET, fluorescence resonance energy transfer; BRET, bioluminescence resonance energy transfer; DTT, dithiothreitol; NEM, *N*-ethylmaleimide.

screening a collection of 73 mutants in which Cys residues were substituted near the extracellular ends of all seven TM regions. Interestingly, cross-links were identified to indicate an interface between the TM1–TM1 dimer and the TM4–TM4 dimer. Thus, although Ste2 is very divergent from mammalian class A GPCRs, the results suggest that the oligomerization interface regions are conserved.

## EXPERIMENTAL PROCEDURES

**Strains and Media.** The *ste2Δ* yeast strain used for the analysis of receptor mutants was yLG123 (*MATa ade2-1<sup>o</sup> his4-580<sup>a</sup> lys2<sup>o</sup> trp1<sup>Δ</sup> tyr1<sup>o</sup> leu2 ura3 SUP4-3<sup>ts</sup> bar1-1 mfa2::FUS1-lacZ ste2::LEU2*). Plasmids carrying wild-type or mutant versions of *STE2* were introduced into yeast using the lithium acetate method, and then the cells were grown in synthetic medium containing adenine and amino acid additives but lacking uracil to select for plasmid maintenance. As described previously (26), a set of Cys substitution mutants was constructed in *STE2* carried in plasmid pJL147 (YE<sub>p</sub>-URA3-*STE2*-T7-3XHA) (27). This plasmid contains a modified *STE2* gene in which the two endogenous Cys residues at positions 59 and 252 were substituted with other amino acids, and it is also C-terminally tagged with a triple HA epitope (28). This modified *STE2* gene displays normal signaling activity and was used as the Cys-minus control receptor for this study.

**Cysteine Cross-Linking.** Cells were grown to log phase in synthetic medium lacking uracil, and then  $\sim 3.5 \times 10^7$  cells were harvested by centrifugation. Cells were washed once in PBS buffer and then resuspended in 500  $\mu$ L of PBS (pH 7.4). Oxidation was initiated by addition of the redox catalyst CuP [Cu(II) (1,10-phenanthroline)<sub>3</sub>] to final concentrations of 500  $\mu$ M Cu and 1.5 M 1,10-phenanthroline, and then the cells were incubated at room temperature for 25 min. The reaction was quenched by addition of EDTA and NEM to final concentrations of 10 mM. The cells were then washed with PBS and collected by centrifugation. For experiments in which the samples were reduced, the oxidized cells were incubated in 200 mM DTT at room temperature for 25 min and then washed with PBS. Cell pellets were stored at  $-80^\circ\text{C}$ . For the time course experiments, the oxidization was terminated at the indicated time points by addition of EDTA and NEM to final concentrations of 10 mM. To examine the effects of ligand binding on cross-linking, cells were first incubated with 10 mM KF and 10 mM NaN<sub>3</sub> at room temperature for 15 min to inhibit receptor endocytosis (29) and then incubated with  $10^{-6}$  M  $\alpha$ -factor for 30 min and oxidized as described above.

**Western Blot Analysis.** Cells were lysed by agitation with glass beads in 400  $\mu$ L of cold lysis buffer [10 mM Tris, 1 mM EDTA, and 10% glycerol (pH 7)] with a protease cocktail (1.5  $\mu$ M pepstatin A, 1 mM benzamide, and 0.5 mM phenylmethanesulfonyl fluoride). Samples were shaken in a Bead Beater for three cycles of agitation for 45 s each, with cooling on ice between cycles. The lysate was cleared by centrifugation at 600g for 18 min at  $4^\circ\text{C}$ . The supernatant was then centrifuged at 18000g for 20 min at  $4^\circ\text{C}$  to spin down the membrane fraction containing Ste2. The membrane fraction was washed with buffer [10 mM Tris and 1 mM EDTA (pH 7)] and then resuspended in SDS gel sample buffer [8 M urea, 4% SDS, and 50 mM Tris (pH 6.8)] for 25 min at room temperature to solubilize Ste2. The samples were then centrifuged at  $22^\circ\text{C}$  and 18000g for 10 min to remove the insoluble particulates before the samples were

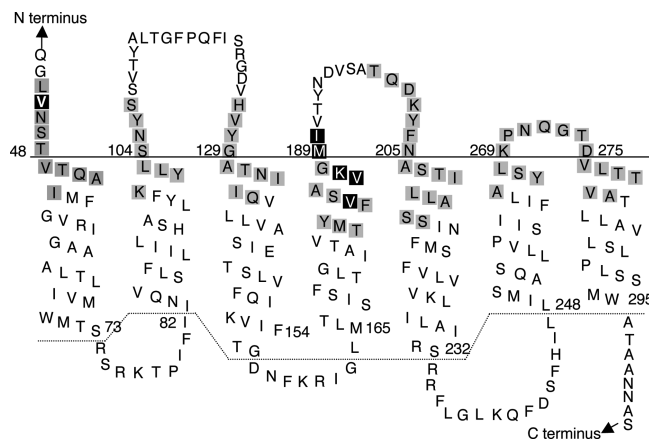


FIGURE 1: Sites of Cys residues introduced near the extracellular ends of the TMs in Ste2. Residues highlighted in black are sites of Cys substitutions that formed disulfide bond-linked dimers, and residues highlighted in gray are sites that did not form disulfide bonds. The topology of Ste2 was predicted on the basis of an assay of the accessibility to a thiol-specific reagent that reacts with solvent-accessible Cys residues but not membrane-embedded Cys (26, 50).

subjected to electrophoresis on a 9% SDS–polyacrylamide gel to separate the Ste2 dimer from the monomer. The gel was then electrophoretically transferred to a nitrocellulose membrane, which was probed with anti-HA monoclonal antibody 12CA5 (Roche Molecular Biochemicals), and then with secondary antibody IRDye 800CW-conjugated goat (polyclonal) anti-mouse IgG. Images were acquired using a digital Odyssey infrared imaging system (LI-COR), and quantitative analysis of the dimer percentage was conducted using Odyssey software.

## RESULTS

**Site-Directed Cys Cross-Linking of Ste2 Dimers.** A Cys cross-linking approach was used to identify amino positions that form the interface between oligomers of Ste2 based on the ability of substituted Cys residues to form intermolecular disulfide bonds. To systematically screen for contact sites, we examined a set of 73 different Ste2 mutants that each contain a Cys substitution near one of the ends of the seven TMs (Figure 1). This set of mutants was constructed previously for mapping the extracellular ends of the TMs based on the accessibility of the Cys residues to a thiol-reactive probe (26, 27). The same set of Cys substitutions was therefore also used in our study to screen for intermolecular disulfide bonds, since residues near the extracellular ends of the TMs are expected to be sensitive to oxidation. Plasmids carrying the receptor mutants were constructed with a modified version of *STE2* in which the endogenous Cys residues were mutated (Cys-minus control) (27, 28). Thus, each Cys substitution mutant in the collection contains only one unique Cys residue. Mutant receptor genes were also modified at the C-terminal coding region to introduce the HA epitope tag to facilitate detection of the mutant proteins. As described previously, only three of the mutants exhibited strong signaling defects (F204C, N205C, and Y266C), but they all produced significant levels of cell surface receptor proteins (26, 27). Four other mutants exhibited slightly decreased levels of receptor signaling but still produced significant levels of cell surface receptors (A52C, L102C, N105C, and A281C) (26, 27).

To screen the collection of mutants for sites of contact between oligomers of Ste2, cells carrying the mutant receptor plasmids were oxidized with 500  $\mu$ M CuP and then analyzed on Western

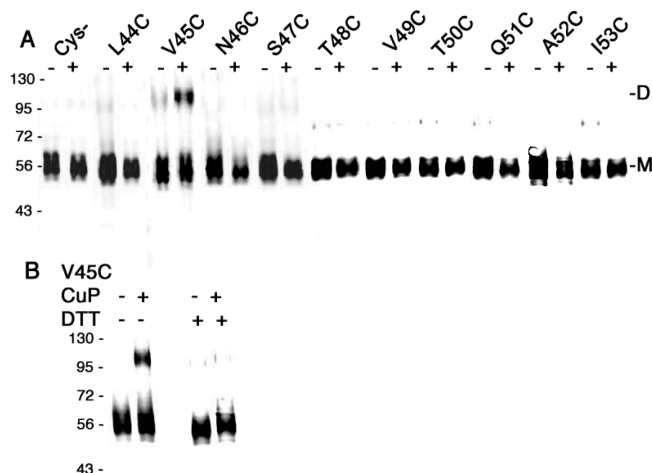


**FIGURE 2:** Analysis of Cys residues near the extracellular end of TM1 for the ability to form disulfide cross-links. (A) Ste2-V45C forms a dimer after oxidation. Ten different Ste2 mutants with Cys residues substituted in place of residues Leu-44–Ile-53 near the extracellular end of TM1 were examined for the ability to form disulfide bonds. Samples were incubated in the absence or presence of the oxidizing agent CuP as indicated, and then the samples were resolved on a 9% SDS–polyacrylamide gel and analyzed on a Western blot probed with anti-HA antibody to detect the presence of Ste2 at either the monomer or dimer position. The blot images were spliced together from different gels to place the mutants in order according to residue number. (B) Dimer formation by the Ste2-V45C mutant was reversed by incubating the sample with the reducing agent DTT (200  $\mu$ M).

blots for gel mobility shifts to indicate the formation of disulfide-bonded Ste2 dimers. This strategy has several advantages over other cross-linking approaches. One is that each cross-link is specific for a unique Cys substituted into Ste2 and does not require further mapping. In addition, a Cys disulfide bond is relatively short ( $\sim 2$  Å) relative to other types of cross-linkers which are usually much longer ( $> 10$  Å). The Cys side chain is also relatively short, so the formation of a cross-link indicates that the  $\alpha$ -carbons of the adjacent molecules of Ste2 are expected to be close in space ( $\leq 7$  Å apart) (30). Control studies demonstrated that a Cys-minus version of Ste2 did not show any significant increase in the extent of dimer formation when incubated under oxidizing conditions (Figure 2). Some SDS-resistant Ste2 dimer formation can occur that is independent of disulfide bond formation, presumably because of hydrophobic aggregation. Therefore, conditions that minimized this type of nonspecific dimer formation were used. As described below, residues in TM1 and TM4 were able to cross-link in response to the oxidizing conditions. In contrast, cross-linking was not observed for Cys residues examined in TM2, TM3, TM5, TM6, and TM7 (data not shown).

**Identification of a Cross-Link near the Extracellular End of TM1.** Ten different mutants that contain Cys residues substituted in place of residues Leu-44–Ile-53 near the extracellular end of TM1 were examined for the ability to form disulfide bonds. After oxidation with CuP, the Cys-minus control and most of the Cys substitution mutant versions of Ste2 still migrated at the monomer position on a Western blot (Figure 2A). Interestingly, the Ste2-V45C mutant exhibited a strong increase in the extent of dimer formation (Figure 2A). This mutant typically showed  $38 \pm 5.6\%$  dimer formation. This was greatly increased relative to  $\sim 3\%$  dimer formation for the Cys-minus control version of Ste2. This percent dimer formation is similar to

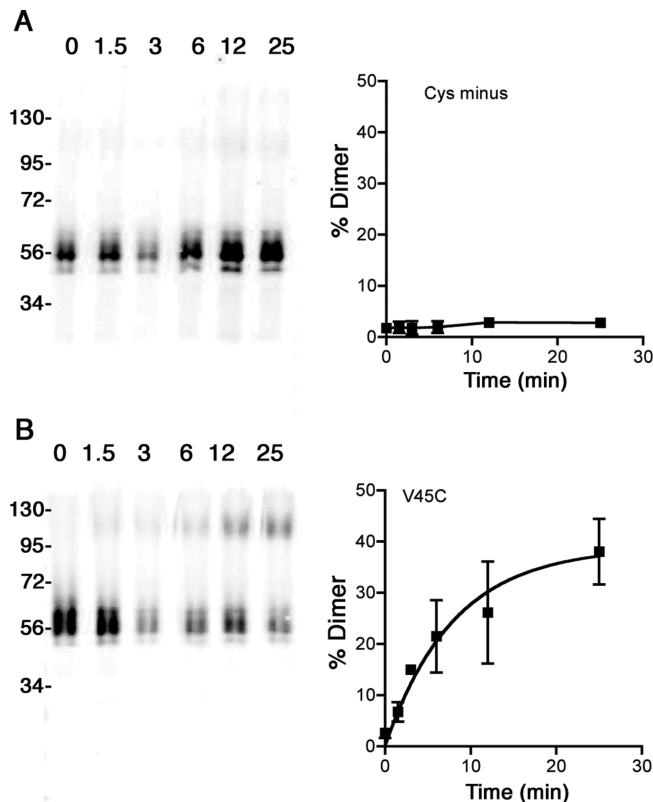


**FIGURE 3:** Time course of dimer formation after oxidation of Ste2-V45C. Cells producing the (A) Ste2-Cys-minus control or (B) Ste2-V45C were oxidized with CuP for the indicated time and then analyzed on Western blots for dimer formation. Quantitative analysis of dimer formation was conducted using a Li-Cor Biosciences Odyssey Infrared Imaging system. Quantitative results for each time point represent the average of two to four different experiments. Error bars indicate the standard deviation.

what has been observed for Cys residues at the interface regions of mammalian GPCRs (13, 14, 31).

To confirm that dimer formation was due to a disulfide bond, we incubated the samples with a reducing agent (200 mM DTT) for 20 min at room temperature. Heating was not used, since it promotes formation of SDS-resistant dimers that are not caused by disulfide bond formation. Following reduction in this manner, the Ste2-V45C mutant migrated primarily as a monomer, confirming that dimer formation was due to a Cys disulfide bond (Figure 2B).

The rate of dimer formation of Ste2-V45C was analyzed in a time course experiment. Samples were oxidized for different amounts of time, blocked with 10 mM NEM and 10 mM EDTA, and then analyzed by Western blotting (Figure 3). The Ste2-V45C mutant formed dimers rapidly with half-maximal dimerization occurring at  $\sim 5.5$  min.

**A Patch of Cys Residues Substituted near the Extracellular End of TM4 Form Cross-Links.** Ten Ste2 mutants with Cys residues substituted near the extracellular end of TM4 (Tyr-181–Ile-190) were oxidized and screened for the ability to form dimers (Figure 4A). Interestingly, Ste2 mutants with Cys residues substituted at five different positions showed a strong increase in the extent of dimer formation. The Ste2-V183C mutant was typically the weakest. The V186C, K187C, M189C, and I190C mutants exhibited stronger ability to form dimers. All of the dimers could be reverted back to monomers following reduction with DTT, confirming that dimer formation was due to a Cys disulfide bond (Figure 4B). Interestingly, as will be



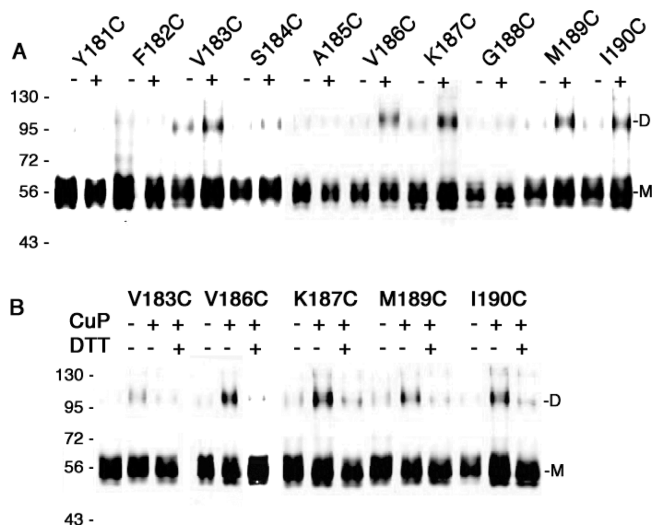


**FIGURE 4:** Analysis of Cys residues near the extracellular end of TM4 for the ability to form disulfide cross-links. (A) Ten Ste2 mutants with Cys residues substituted in place of residues Tyr-181–Ile-190 near the extracellular end of TM4 were oxidized with CuP and then analyzed on Western blots probed with anti-HA for dimer formation. Note that Ste2 mutants with Cys residues substituted at five different positions exhibited a strong increase in the extent of dimer formation, including the V183C, V186C, K187C, M189C, and I190C mutant versions of Ste2. The blot images were spliced together from different gels to place the mutants in order according to residue number. (B) Ste2 dimers were reverted back to monomers following reduction with DTT, confirming that dimer formation was due to a Cys disulfide bond.

described in Discussion, this set of Ste2 residues is predicted to fall on one face of an  $\alpha$ -helical representation of TM4.

Analysis of a time course of oxidation showed that the V183C, V186C, K187C, and I190C Ste2 mutants all formed dimers with a half maximal time of  $\sim 2$  min (Figure 5). In contrast, the half-maximal time for dimer formation was slightly slower for the M189C mutant (4.8 min). Perhaps the kinetics are slower for M189C because it is farthest from the main cluster of positions where Cys substitutions form cross-links (see Discussion).

These results represent strong evidence that residues at the extracellular end of TM4 form contacts in Ste2. The greater number of positions that were able to cross-link at the end of TM4 relative to only one position at the end of TM1 is also interesting. This suggests that this region of TM4 may be more flexible or may form a more extensive contact in the dimer than TM1 does. The identification of TM4 as a site of oligomer contact for Ste2 is also very significant because it suggests that this feature is highly conserved among GPCRs. TM4 homomeric contacts have been reported in very divergent members of the GPCR family, including mammalian class A GPCRs (13, 14, 16).

**Effects of Ligand Binding on Cross-Linking.** Cross-linking of the Cys residues in TM1 and TM4 was examined in the presence and absence of  $\alpha$ -factor to determine the effects of ligand binding on the sites and efficiency of dimer formation. Ligand binding could alter the efficiency with which Ste2 monomers associate, or it could change the spatial arrangement of residues to promote new contact sites. Incubation of TM1 mutants with  $\alpha$ -factor did not reveal any new contact sites. Ste2-V45C was still the only TM1 mutant that formed dimers efficiently (Figure 6A). Quantitative analysis did not reveal any significant differences in the efficiency of Ste2-V45C dimer formation in the presence or absence of  $\alpha$ -factor (Figure 7).

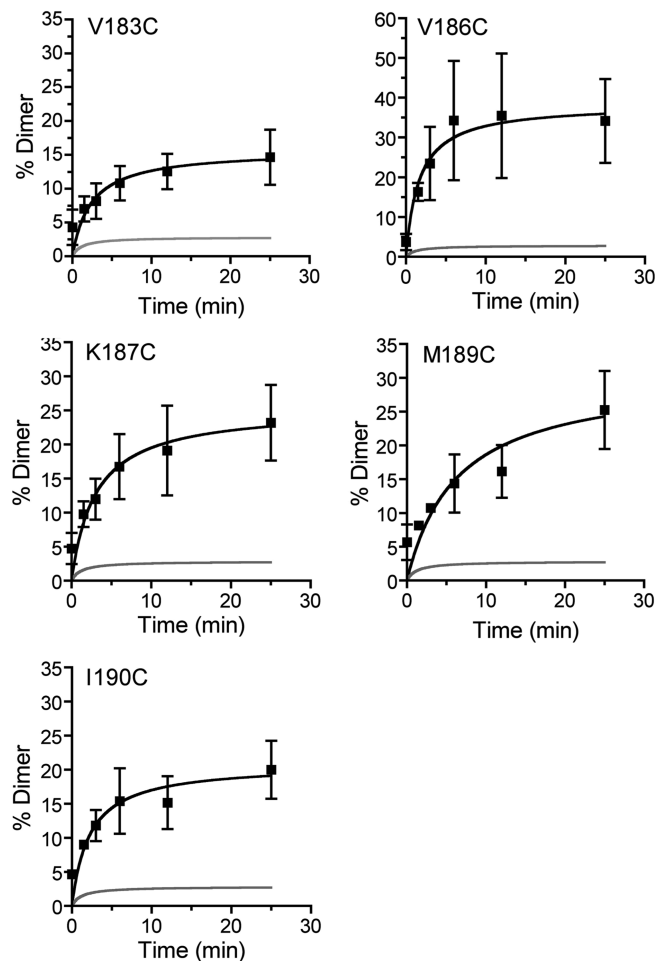


**FIGURE 5:** Time course of dimer formation after oxidation of Ste2 mutants with substitutions near the extracellular end of TM4. The V183C, V186C, K187C, M189C, and I190C mutant versions of Ste2 were oxidized with CuP for the indicated time and then analyzed on Western blots for dimer formation. For the sake of comparison, the curve for the control Cys-minus version of Ste2 is shown as a gray line. Quantitative analysis of dimer formation was conducted using a Li-Cor Biosciences Odyssey Infrared Imaging system as described in Experimental Procedures. Results represent the average of two to six independent experiments. Error bars indicate the standard deviation.

Analysis of the TM4 mutants in the presence of  $\alpha$ -factor also did not reveal any new sites of contact (Figure 6B). The same five mutant versions of Ste2 that cross-linked in the absence of  $\alpha$ -factor (V183C, V186C, K187C, M189C, and I190C) were still the only mutants that exhibited a significant increase in the level of dimers after oxidation in the presence of  $\alpha$ -factor. The efficiency of cross-linking for V186C, K187C, M189C, and I190C mutants was not changed significantly in the presence of  $\alpha$ -factor. However, quantitative analysis of Ste2-V183C revealed an increase in the extent of dimer formation in the presence of  $\alpha$ -factor (Figure 7). In an average of five assays, the level of Ste2-V183C dimer formation increased from 21.2 to 33.4% in the presence of  $\alpha$ -factor ( $p = 0.024$ ). Incubation with  $\alpha$ -factor caused an increase in the level of dimer formation in all five independent assays.

## DISCUSSION

Formation of GPCR dimers or oligomers is thought to play important roles in receptor biogenesis, trafficking, and signaling (6–9). However, contact sites between the monomers are

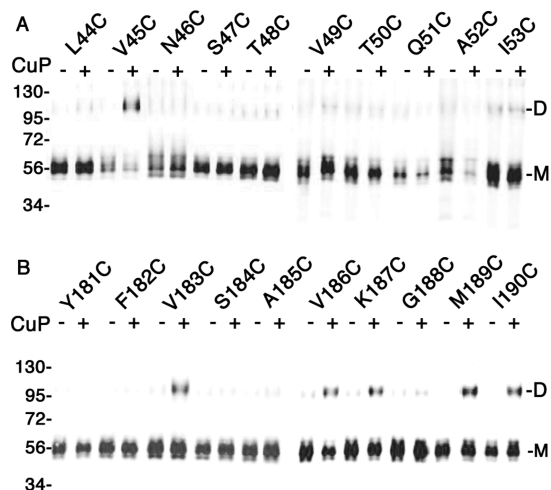


FIGURE 6: Ste2 dimerization in the presence of  $\alpha$ -factor. The Ste2 mutants with Cys residues substituted near the extracellular end of (A) TM1 and (B) TM4 were incubated in the presence of  $10^{-6}$  M  $\alpha$ -factor for 30 min and then oxidized with CuP. The plus and minus symbols above each lane indicate whether the samples were oxidized with CuP. Samples were analyzed on Western blots probed with anti-HA. The blot images were spliced together from different gels to place the mutants in order according to residue number.

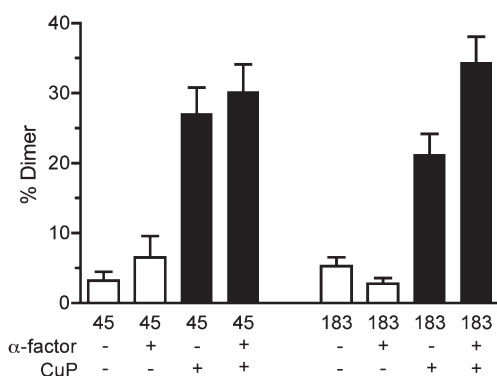


FIGURE 7: Increased extent of dimer formation for Ste2-V183C in the presence of  $\alpha$ -factor. Quantitative analysis of the efficiency of dimer formation for Ste2-V45C and Ste2-V183C in the presence and absence of  $\alpha$ -factor. Results represent the average of four to five independent experiments. Error bars indicate the standard deviation.

poorly defined. Therefore, in this study, we examined a set of 73 Cys substitution mutants of the  $\alpha$ -factor receptor (Ste2) for the ability to form homomeric disulfide bonds. These studies were conducted in the normal cellular membranes and did not require detergent extraction and purification, which could alter receptor structure. The results indicate that contacts form between the TM1–TM1 dimer and the TM4–TM4 dimer in Ste2. This provides the first direct evidence for the involvement of TM4 as a contact site in Ste2 oligomers. In addition, these results also identify the positions of residues involved in the oligomer interface. As described below, these new data on the interface sites in Ste2 oligomers reveal common features of receptor oligomerization that are conserved across the diverse GPCR family (10, 13).

**Homomeric TM1 Contacts in Ste2 and Other GPCR Oligomers.** The ability of Ste2-V45C to form disulfide-bonded dimers (Figures 2 and 3) indicates that residues near the extracellular end of TM1 form an interface site. Contact between TM1 domains in Ste2 dimers is in agreement with previous FRET studies, which implicated a region including the N-terminus and TM1 in forming dimers (32). Further FRET analysis implicated a

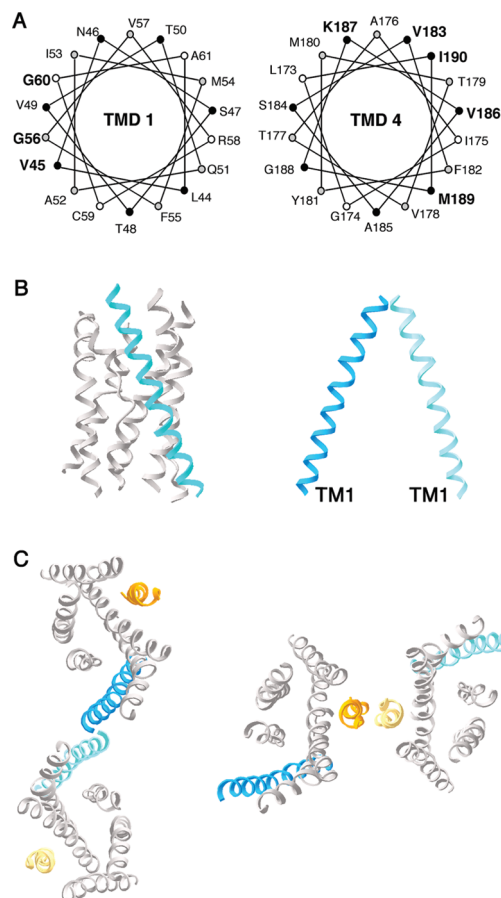


FIGURE 8: Models for the interaction of Ste2 dimers. (A) Models of  $\alpha$ -helix formation for the extracellular ends of TM1 and TM4 with positions involved in dimer formation shown in bold. Note that Val-45 in TM1 and the cluster of residues involved in dimer formation near the end of TM4 are predicted to face away from the helix bundle. (B) Ribbon model of TM helices of rhodopsin (Protein Data Bank entry 1L9H) with TM1 colored to help reveal its tilt relative to the other TMs. On the right, two TM1 helices are docked in the approximate position that would be expected for a cross-link at V45C in Ste2. (C) Extracellular view of GPCR helix bundles forming a dimer with contact at TM1 on the left and contact at TM4 on the right. Note that TM1 and TM4 contacts are too far apart to form contacts in the same dimer.

GxxxG sequence involving Gly-56 and Gly-60 in the middle region of Ste2 TM1 as forming a glycophorin-type motif that could stabilize the interaction between the TM1 helices (33). A helical wheel prediction for the  $\alpha$ -helical structure of TM1 predicts that Val-45, Gly-56, and Gly-60 would all fall on the face of TM1 that is generally predicted to face away from the helix bundle (Figure 8A). However, if TM1 of Ste2 is tilted in the plane of the membrane, as it is in the high-resolution structures of several class A GPCRs, including rhodopsin, A2a-adenosine, and  $\beta$ -adrenergic receptors (34–38), it would not be possible to form contacts at both the GxxxG motif in the middle of TM1 and Val-45 at the extracellular side of TM1 (Figure 8B). Furthermore, the  $40^\circ$  tilt of the helices in glycophorin A dimers (39) also makes it unlikely that the extracellular ends of TM1 would be in the proximity in this type of configuration. This suggests that the GxxxG motif may be important for the proper structure of TM1, but it may not form a direct contact in the dimer. Alternatively, there may be flexibility in TM1 or a distinct structure in this region of Ste2 that permits contact at both the GxxxG motif and the extracellular end where Cys cross-linking occurs.

Residues that form dimer contact sites involving the extracellular end of TM1 have also been detected by cross-linking studies with other GPCRs, including the D2-dopamine receptor (13) and the 5HT2c serotonin receptor (14). Disulfide bond formation was detected for Cys residues substituted at a cluster of four positions at the extracellular end of TM1 in the D2-dopamine receptor (residues 36, 37, 40, and 43) and for a cluster of five residues that span the extracellular boundary of TM1 in the 5HT2c receptor (residues 50–52, 55, and 56) (13, 14). Since the dopamine and serotonin receptors are in the class A family along with rhodopsin, TM1 is expected to be tilted in the plane of the membrane as shown in Figure 8B. In addition, a model based on atomic force microscopy analysis of rhodopsin also suggests that the extracellular ends of TM1 interact (10). Thus, contact between residues at the extracellular end of TM1 is a conserved feature of oligomers for both class A GPCRs and the very divergent class D Ste2 pheromone receptor.

**TM4 Homomeric Contacts.** Five different positions at the extracellular end of TM4 in Ste2 showed a strong increase in dimer formation after oxidation (V183C, V186C, K187C, M189C, and I190C) (Figures 4 and 5). TM4 has not previously been proposed to be a specific contact site for Ste2 oligomer formation, although FRET analysis of Ste2 subfragments suggested that there could be a second interface in the region encompassing TM4–TM7 (32). Mapping of the five residues that were involved in forming dimers onto a helical wheel prediction for  $\alpha$ -helical structure of TM4 indicates that all of these residues fall on one side of TM4 (Figure 8A). Interestingly, this side of TM4 is predicted to face away from the monomer helix bundle (5), consistent with these residues forming part of the oligomer interface. None of the residues in the extracellular end of TM4 are highly conserved in Ste2 proteins produced by other fungal species (5), suggesting that the TM4 interface forms via general contacts and is not obviously mediated by a specific amino acid motif. Consistent with this, scanning mutagenesis and targeted random mutagenesis of this region of TM4 did not identify mutations that cause significant phenotypic consequences (26, 40), although two strong loss-of-function mutations were identified in other studies that are caused by rather dramatic S184R and A185P substitutions in Ste2 (41, 42).

Residues near the extracellular end of TM4 were also found to form a dimer interface region in class A GPCRs. Cross-linking analysis of selected Cys substitutions in opsin showed that a Cys at the extracellular end of TM4 (W175C) could form a disulfide bond (16). Similarly, Cys168 at a similar position near the end of TM4 in the D2-dopamine receptor could cross-link (31). TM4 is also predicted to form a contact for the C5a receptor (15). Perhaps more contacts in this interface region would have been identified in these other GPCRs if more Cys substitutions were examined, similar to the results for Ste2. Interestingly, in the case of the 5HT2c receptor, cross-links were detected between combinations of Cys residues at the extracellular ends of TM4 and TM5 (14). Thus, TM4 acts as an interface site in a wide range of GPCRs.

**Ligand-Induced Changes in Receptor Oligomerization.** Changes in cross-linking patterns in response to ligand can be used to identify structural changes that occur at the oligomer interface. Analysis of Cys residues substituted into TM1 failed to detect any differences; Ste2-V45C was still the only mutant that displayed dimer formation after oxidation (Figure 6A). Interestingly, the extracellular end of TM1 in Ste2 has also been implicated as a contact site for its ligand,  $\alpha$ -factor (43).

This suggests that although TM1 participates in ligand binding, the interaction with  $\alpha$ -factor does not cause a major conformational change in the TM1 interface region of Ste2 oligomers. Similar results were reported for the D2-dopamine receptor (13) and for the 5HT2c serotonin receptor (14), in which no change in Cys cross-linking was observed for TM1 residues after ligand binding.

Binding of the  $\alpha$ -factor ligand also did not cause a change in which Cys residues substituted into TM4 could form dimers after oxidation (Figure 6B). However, quantitative analysis indicated that ligand binding increased the efficiency of dimer formation for Ste2-V183C (Figure 7). Of the five positions in TM4 that formed disulfide bonds, Val-183 is the most deeply buried in the membrane (Figure 1). This suggests that portions of TM4 may undergo a change in conformation in response to ligand binding. In this regard, it is interesting that several substitution mutations in Ste2 that cause defects in signaling have been identified that affect this region of TM4, including those that cause a dominant-negative phenotype (41, 42, 44). Alternatively, it is also possible that the increased level of dimer formation for Ste2-V183C is due to ligand-induced stabilization of oligomers (45).

**Monomer Model of Ste2.** The identification of dimer contact sites in Ste2 not only helps to map the oligomer interface but also contributes to an improved understanding of the Ste2 monomer. The structure of Ste2 is less well understood than some of the other GPCRs for which high-resolution structures are available. Ste2 is also too divergent for detailed homology modeling with the class A GPCRs whose structure is known. Thus, it is significant that Ste2-V45C forms dimers, since it provides additional support for models proposing that the corresponding side of TM1 faces away from the helix bundle (5). Similarly, the identification of residues in TM4 that form the oligomer interface also helps to determine the proper orientation of TM4 in the monomer helix bundle of Ste2. This information is particularly helpful for modeling the orientation of TM4, since there are no strongly polar residues or other features to help provide a guide for the proper orientation of this transmembrane helix.

**Oligomer Model.** The Cys cross-linking studies indicate that Ste2 is similar to class A GPCRs in that both TM1 and TM4 can form homomeric interface sites in oligomers (13–15). These cross-linking data for the class A GPCRs are also supported by other types of analyses, such as atomic force microscopy and electron cryomicroscopy, which indicate that the packing arrangement of rhodopsin in membranes also involves interfaces between TM1 and TM4 (10–12). This suggests important conservation of the oligomerization interface regions across widely divergent GPCRs that show no obvious sequence identity. However, Ste2 may not form an identical oligomer arrangement, since oxidation of Cys residues substituted into the extracellular end of Ste2 TM5 did not form dimers, as was observed for the Y206C substitution at the extracellular end of TM5 in opsin (16).

The detection of homomeric contacts for both TM1 and TM4 suggests that Ste2 forms oligomers and not just dimers. Modeling of the contact sites using the crystal structure of rhodopsin indicates that the corresponding regions are too far apart for TM1–TM1 and TM4–TM4 homomeric contacts to form in the same dimer (Figure 8C). Similar conclusions with regard to separate contact sites in oligomers of class A GPCRs were proposed previously on the basis of the distance between TM1 and TM4 (10, 13, 15). Thus, since the seven TMs of Ste2 are



thought to form a helix bundle with the same general arrangement as rhodopsin (5, 28, 46, 47), Ste2 is also likely to form oligomers and not just dimers in vivo. A recent FRET study came to the opposite conclusion and suggested that Ste2 exists only as dimers (25). However, it is possible that FRET could detect only one type of Ste2 dimer interface in this study since the fluorescent proteins used as FRET donors and acceptors were fused to the end of TM7.

Another interesting aspect of the identification of TM1 and TM4 as sites of dimer contact is that these TMs are not predicted to move much during rhodopsin activation (48, 49). TM1–TM4 are thought to form a core structure that interacts with TM5–TM7, which are predicted to undergo movement during receptor activation. Thus, sites of dimer contact at TM1 and TM4 may be conserved in divergent GPCRs from yeast to humans as part of an underlying mechanism to permit oligomers to form without constraining the ability of the TMs to undergo conformational changes during receptor activation.

## ACKNOWLEDGMENT

We thank Lois Douglas and Chengda Zhang for assistance with developing the experimental methods. We also thank the previous members of our lab who were involved in constructing the Cys substitution mutants and Lois Douglas and Markus Eilers for helpful comments on the manuscript.

## REFERENCES

- Kristiansen, K. (2004) Molecular mechanisms of ligand binding, signaling, and regulation within the superfamily of G-protein-coupled receptors: Molecular modeling and mutagenesis approaches to receptor structure and function. *Pharmacol. Ther.* 103, 21–80.
- Gether, U. (2000) Uncovering molecular mechanisms involved in activation of G protein-coupled receptors. *Endocrin. Rev.* 21, 90–113.
- Kolakowski, L. F. Jr. (1994) GCRDB: A G-protein-coupled receptor database. *Receptors Channels* 2, 1–7.
- Probst, W. C., Snyder, L. A., Schuster, D. I., Brosius, J., and Sealfon, S. C. (1992) Sequence alignment of the G-protein coupled receptor superfamily. *DNA Cell Biol.* 11, 1–20.
- Eilers, M., Hornak, V., Smith, S. O., and Konopka, J. B. (2005) Comparison of Class A and D G Protein-Coupled Receptors: Common Features in Structure and Activation. *Biochemistry* 44, 8959–8975.
- Terrillon, S., and Bouvier, M. (2004) Roles of G-protein-coupled receptor dimerization. *EMBO Rep.* 5, 30–34.
- Bulenger, S., Marullo, S., and Bouvier, M. (2005) Emerging role of homo- and heterodimerization in G-protein-coupled receptor biosynthesis and maturation. *Trends Pharmacol. Sci.* 26, 131–137.
- Park, P. S., Filipek, S., Wells, J. W., and Palczewski, K. (2004) Oligomerization of G protein-coupled receptors: Past, present, and future. *Biochemistry* 43, 15643–15656.
- Overton, M. C., Chinault, S. L., and Blumer, K. J. (2005) Oligomerization of G-protein-coupled receptors: Lessons from the yeast *Saccharomyces cerevisiae*. *Eukaryotic Cell* 4, 1963–1970.
- Liang, Y., Fotiadis, D., Filipek, S., Saperstein, D. A., Palczewski, K., and Engel, A. (2003) Organization of the G protein-coupled receptors rhodopsin and opsin in native membranes. *J. Biol. Chem.* 278, 21655–21662.
- Fotiadis, D., Liang, Y., Filipek, S., Saperstein, D. A., Engel, A., and Palczewski, K. (2003) Atomic-force microscopy: Rhodopsin dimers in native disc membranes. *Nature* 421, 127–128.
- Davies, A., Gowen, B. E., Krebs, A. M., Schertler, G. F., and Saibil, H. R. (2001) Three-dimensional structure of an invertebrate rhodopsin and basis for ordered alignment in the photoreceptor membrane. *J. Mol. Biol.* 314, 455–463.
- Guo, W., Urizar, E., Kralikova, M., Mobarec, J. C., Shi, L., Filizola, M., and Javitch, J. A. (2008) Dopamine D2 receptors form higher order oligomers at physiological expression levels. *EMBO J.* 27, 2293–2304.
- Mancia, F., Assur, Z., Herman, A. G., Siegel, R., and Hendrickson, W. A. (2008) Ligand sensitivity in dimeric associations of the serotonin 5HT2c receptor. *EMBO Rep.* 9, 363–369.
- Klco, J. M., Lassere, T. B., and Baranski, T. J. (2003) C5a receptor oligomerization. I. Disulfide trapping reveals oligomers and potential contact surfaces in a G protein-coupled receptor. *J. Biol. Chem.* 278, 35345–35353.
- Kota, P., Reeves, P. J., Rajbhandary, U. L., and Khorana, H. G. (2006) Opsin is present as dimers in COS1 cells: Identification of amino acids at the dimeric interface. *Proc. Natl. Acad. Sci. U.S.A.* 103, 3054–3059.
- Brock, C., Oueslati, N., Soler, S., Boudier, L., Rondard, P., and Pin, J. P. (2007) Activation of a dimeric metabotropic glutamate receptor by intersubunit rearrangement. *J. Biol. Chem.* 282, 33000–33008.
- Whorton, M. R., Jastrzebska, B., Park, P. S., Fotiadis, D., Engel, A., Palczewski, K., and Sunahara, R. K. (2008) Efficient coupling of transducin to monomeric rhodopsin in a phospholipid bilayer. *J. Biol. Chem.* 283, 4387–4394.
- Whorton, M. R., Bokoch, M. P., Rasmussen, S. G., Huang, B., Zare, R. N., Kobilka, B., and Sunahara, R. K. (2007) A monomeric G protein-coupled receptor isolated in a high-density lipoprotein particle efficiently activates its G protein. *Proc. Natl. Acad. Sci. U.S.A.* 104, 7682–7687.
- Falke, J. J., and Hazelbauer, G. L. (2001) Transmembrane signaling in bacterial chemoreceptors. *Trends Biochem. Sci.* 26, 257–265.
- Frillingos, S., Sahin-Toth, M., Wu, J., and Kaback, H. R. (1998) Cys-scanning mutagenesis: A novel approach to structure function relationships in polytopic membrane proteins. *FASEB J.* 12, 1281–1299.
- Kaback, H. R., Sahin-Toth, M., and Weinglass, A. B. (2001) The kamikaze approach to membrane transport. *Nat. Rev. Mol. Cell Biol.* 2, 610–620.
- Gehret, A. U., Bajaj, A., Naider, F., and Dumont, M. E. (2006) Oligomerization of the yeast  $\alpha$ -factor receptor: Implications for dominant negative effects of mutant receptors. *J. Biol. Chem.* 281, 20698–20714.
- Overton, M. C., and Blumer, K. J. (2000) G-protein-coupled receptors function as oligomers in vivo. *Curr. Biol.* 10, 341–344.
- Raicu, V., Jansma, D. B., Miller, R. J., and Friesen, J. D. (2005) Protein interaction quantified in vivo by spectrally resolved fluorescence resonance energy transfer. *Biochem. J.* 385, 265–277.
- Lin, J. C., Duell, K., and Konopka, J. B. (2004) A microdomain formed by the extracellular ends of the transmembrane domains promotes activation of the G protein-coupled  $\alpha$ -factor receptor. *Mol. Cell. Biol.* 24, 2041–2051.
- Lin, J., Parrish, W., Eilers, M., Smith, S. O., and Konopka, J. B. (2003) Aromatic residues at the extracellular ends of transmembrane domains 5 and 6 are important for ligand activation of the G protein-coupled  $\alpha$ -factor receptor. *Biochemistry* 42, 293–301.
- Dube, P., DeConstanzo, A., and Konopka, J. B. (2000) Interaction between transmembrane domains 5 and 6 in the  $\alpha$ -factor receptor. *J. Biol. Chem.* 275, 26492–26499.
- Jenness, D. D., and Spatrick, P. (1986) Down regulation of the  $\alpha$ -factor pheromone receptor in *Saccharomyces cerevisiae*. *Cell* 46, 345–353.
- Falke, J. J., Dernburg, A. F., Sternberg, D. A., Zalkin, N., Milligan, D. L., and Koshland, D. E. Jr. (1988) Structure of a bacterial sensory receptor. A site-directed sulfhydryl study. *J. Biol. Chem.* 263, 14850–14858.
- Guo, W., Shi, L., and Javitch, J. A. (2003) The fourth transmembrane segment forms the interface of the dopamine D2 receptor homodimer. *J. Biol. Chem.* 278, 4385–4388.
- Overton, M. C., and Blumer, K. J. (2002) The extracellular N-terminal domain and transmembrane domains 1 and 2 mediate oligomerization of a yeast G protein-coupled receptor. *J. Biol. Chem.* 277, 41463–41472.
- Overton, M. C., Chinault, S. L., and Blumer, K. J. (2003) Oligomerization, biogenesis, and signaling is promoted by a glycophorin A-like dimerization motif in transmembrane domain 1 of a yeast G protein-coupled receptor. *J. Biol. Chem.* 278, 49369–49377.
- Palczewski, K., Kumasaka, T., Hori, T., Behnke, C. A., Motoshima, H., Fox, B. A., Le Trong, I., Teller, D. C., Okada, T., Stenkamp, R. E., Yamamoto, M., and Miyano, M. (2000) Crystal structure of rhodopsin: A G protein-coupled receptor. *Science* 289, 739–745.
- Jaakola, V. P., Griffith, M. T., Hanson, M. A., Cherezov, V., Chien, E. Y., Lane, J. R., Ijzerman, A. P., and Stevens, R. C. (2008) The 2.6 angstrom crystal structure of a human  $A_{2A}$  adenosine receptor bound to an antagonist. *Science* 322, 1211–1217.
- Warne, T., Serrano-Vega, M. J., Baker, J. G., Moukhametzianov, R., Edwards, P. C., Henderson, R., Leslie, A. G., Tate, C. G., and Schertler, G. F. (2008) Structure of a  $\beta$ 1-adrenergic G-protein-coupled receptor. *Nature* 454, 486–491.

37. Rasmussen, S. G., Choi, H. J., Rosenbaum, D. M., Kobilka, T. S., Thian, F. S., Edwards, P. C., Burghammer, M., Ratnala, V. R., Sanishvili, R., Fischetti, R. F., Schertler, G. F., Weis, W. I., and Kobilka, B. K. (2007) Crystal structure of the human  $\beta$ 2 adrenergic G-protein-coupled receptor. *Nature* 450, 383–387.
38. Cherezov, V., Rosenbaum, D. M., Hanson, M. A., Rasmussen, S. G., Thian, F. S., Kobilka, T. S., Choi, H. J., Kuhn, P., Weis, W. I., Kobilka, B. K., and Stevens, R. C. (2007) High-resolution crystal structure of an engineered human  $\beta$ 2-adrenergic G protein-coupled receptor. *Science* 318, 1258–1265.
39. MacKenzie, K. R., Prestegard, J. H., and Engelman, D. M. (1997) A transmembrane helix dimer: Structure and implications. *Science* 276, 131–133.
40. Martin, N. P., Celic, A., and Dumont, M. E. (2002) Mutagenic mapping of helical structures in the transmembrane segments of the yeast  $\alpha$ -factor receptor. *J. Mol. Biol.* 317, 765–788.
41. Dosil, M., Giot, L., Davis, C., and Konopka, J. B. (1998) Dominant-negative mutations in the G protein-coupled  $\alpha$ -factor receptor map to the extracellular ends of the transmembrane segments. *Mol. Cell. Biol.* 18, 5981–5991.
42. Schandel, K. A., and Jenness, D. D. (1994) Direct evidence for ligand-induced internalization of the yeast  $\alpha$ -factor pheromone receptor. *Mol. Cell. Biol.* 14, 7245–7255.
43. Son, C. D., Sargsyan, H., Naider, F., and Becker, J. M. (2004) Identification of ligand binding regions of the *Saccharomyces cerevisiae*  $\alpha$ -factor pheromone receptor by photoaffinity cross-linking. *Biochemistry* 43, 13193–13203.
44. Leavitt, L. M., Macaluso, C. R., Kim, K. S., Martin, N. P., and Dumont, M. E. (1999) Dominant negative mutations in the  $\alpha$ -factor receptor, a G protein-coupled receptor encoded by the *STE2* gene of the yeast *Saccharomyces cerevisiae*. *Mol. Gen. Genet.* 261, 917–932.
45. Shi, C., Paige, M. F., Maley, J., and Loewen, M. C. (2009) In vitro characterization of ligand-induced oligomerization of the *S. cerevisiae* G-protein coupled receptor, Ste2p. *Biochim. Biophys. Acta* 1790, 1–7.
46. Lee, Y. H., Naider, F., and Becker, J. M. (2006) Interacting residues in an activated state of a G protein-coupled receptor. *J. Biol. Chem.* 281, 2263–2272.
47. Naider, F., Estephan, R., Englander, J., Suresh Babu, V. V., Arevalo, E., Samples, K., and Becker, J. M. (2004) Sexual conjugation in yeast: A paradigm to study G-protein-coupled receptor domain structure. *Biopolymers* 76, 119–128.
48. Liu, W., Eilers, M., Patel, A. B., and Smith, S. O. (2004) Helix packing moments reveal diversity and conservation in membrane protein structure. *J. Mol. Biol.* 337, 713–729.
49. Patel, A. B., Crocker, E., Reeves, P. J., Getmanova, E. V., Eilers, M., Khorana, H. G., and Smith, S. O. (2005) Changes in interhelical hydrogen bonding upon rhodopsin activation. *J. Mol. Biol.* 347, 803–812.
50. Choi, Y., and Konopka, J. B. (2006) Accessibility of Cys residues substituted into the cytoplasmic regions of the  $\alpha$ -factor receptor identifies the intracellular residues that are available for G protein interaction. *Biochemistry* 45, 15310–15317.